Supplementary Information

1. Materials and Methods

1.1. Brain network construction

Generally, network analysis consist of two important elements - **nodes** and **edges**. These two elements are the building blocks of networks and their accurate definitions are very important for any network model [1] and also applicable to network neuroscience. The standard method of defining nodes in neuroimaging, particularly for fMRI studies is by the structural atlas or parcellation of brain structure into different regions. The nodes are usually represented by collection of voxels within the defined structure and the edges are the statistical dependences of the brain activity of the pair of nodes. In this study, the brain is parcellated into 112 subcortical and cortical regions (see supplementary Table 1) defines by structural Harvard-Oxford atlas of the fMRIB [2, 3]. Each regions is represented by average of voxel time series within in the region.

The edge weights that link the brain nodes (regions) were calculated by the wavelet transform coherence (WTC) [4], smoothed over time and frequency to avoid bias toward unity coherence. We derived the spectral estimates of the time series using Morlet wavelets defined w(t,f) as :

$$w(t,f) = (\sigma_t \sqrt(\pi))^{-\frac{1}{2}} e^{-i2\pi f t} e^{-\frac{t^2}{2\sigma_t^2}} \tag{1}$$

Here, f is the centre frequency and σ_t is the temporal standard deviation. The time-frequency estimate, X(t,f) of time series x(t) was computed by the convolution with wavelet coefficients, w(t,f);

$$X(t,f) = x(t) * w(t,f) \tag{2}$$

We selected the central frequency of 1/12 Hz corresponding to spectral width of 0.05 to 0.11Hz for full width at half maximum(FWHM) . Therefore, the wavelet transform coherence between two regions x and y is defined as followed [4, 5, 6]:

$$WTC^2(f,t) = \frac{|S(s^{-1}X_{xy}(t,f)|^2}{S(s^{-1}|X_x(t,f)|^2) \cdot S(s^{-1}|X_y(t,f)|^2)} \tag{3}$$

Where X_{xy} is the cross-wavelet of X_x and X_y, s is the scale which depend on the frequency [5, 6] and S is the smoothing operator. This definition closely resembles that of a traditional coherence but the wavelet coherence is localized correlation coefficient in both time and frequency space. Higher scales are required for lower frequency signals [5, 6] and in this study, we used scale of s=32 for the smoothing operation. This procedure was repeated for all pair of regions yielding adjacency matrix, **A**, with 112 by 112 dimensions which is the representative of functional connectvity between the brain regions.

1.2. Network modularity

Network modularity is one of the concept of network neuroscience to characterized the brain nodes into modules or *communities* by using community detections algorithms [7]. A community of nodes is group of nodes that are more connected not only by region but also by their functional similarity . The common method of community detection algorithms is the optimization of nodes partition into modules. In this study, we implemented a generalized Louvain detection algorithms [8, 9] which considers multiple adjacency matrices as slices of network. The multislice system was implemented by all adjacency matrices of all scans and subjects during the period of value learning task. The quality function, **Q**, which used intra-community and inter-community connections to identify a partition of networks nodes [9] is defined as :

$$Q = \frac{1}{2\mu}\sum_{ijs}[(A_{ijs} - \gamma_s V_{ijs})\delta_{sr} + \delta_{ij}\omega_{jsr}]\delta(g_{is}, g_{jr}) \tag{4}$$

Where A_{ijs} is the components of adjacency matrix of slice, s, and element $Vijs$ is the component of the null model matrix tuned by the structural resolution γ. In this study, the γ standard parameter of 1 is selected. We employed the Newman-Girvan null model within each layer by using $V_{ijs} = \frac{k_{is}k_{js}}{2m_s}$, where k is the total edge weight and m_s is the total edges weight in slice , s. The interslice coupling parameter, ω_{jsr} is the connection strength between node j in slice s and node j in slice r and the total edge in the network is $\mu = \frac{1}{2}\sum_{jr}\kappa_{jr}$. The strength of the node, κ_{jr} is the sum of intraslice strength and interslice: $\kappa_{jr} = k_{jr} + c_{jr}$, and $c_{jr} = \sum_s \omega_{jrs}$ However, in our study we fixed this parameter to be $\omega = 1$. The last part of the equation 4 is the community assignments and $\delta(gi, gj) = 1$ if g_i and g_j of nodes i and j are the same and 0 otherwise. We obtained partition of brain into network communities for each scan and subject with the standard parameter of $\gamma = \omega = 1$. We obtained the module allegiance matrix [10], whose elements correspond to the probability that two regions belong to the same community across all the scans and subjects. The seven network communities generated with this procedure are as shown in Table 1 (in the main text).

1.3. Inter-subject correlation (ISC) and inter-subject functional connectivity (ISFC)

We have shown in the main article how we obtained ISC and ISFC. ISC measured the reliability of stimulus driven responses across the subjects and allows the detection of all sensory cortical regions without assumptions or a priori knowledge of the temporal composition of exact cortical responses. However, we measures the reliability of ISC by computing the Pearson correlation between each subject three scans for each day to confirmed the ISC within subject. This was performed on bold time series signals on region-by-region. Each correlation value for each scan and subject was converted to Z score value to enable comparison with other scans and subjects.

Similarly, we estimated the consistency of the FC by computing the edge persistence [11] of the brain network across the three runs for each day to established the reliability of ISFC within subject . The edge persistence measures the topological overlap of the neighborhood from one scan to another by estimating the probability that nodes connected at a scan 1 will still be connected during scan 2 . For the three scans (s1,s2 and s3) in each day, the edge persistence is defined as:

$$C_i(s_1, s_2, s_3) = \frac{\sum_j a_{ij}(s_1)a_{ij}(s_2)a_{ij}(s_3)}{\sqrt{([\sum_j a_{ij}(s_1)][\sum_j a_{ij}(s_2)][\sum_j a_{ij}(s_3)])}} \quad (5)$$

Where a_{ij} is the edge strength between of node i and j from the adjacency functional matrix, A and C_i is the edge persistence for node i.

1.4. Edge strength and Resistivity

In order to determine the brain regions that mostly impact the brain network performance during the value learning task, we investigated the regions with high degree by computing the edge strength (or degree) and resistivity . A region with higher degree is said to be of very important for the system network performance. The edge strength is defined as

$$S(i) = \frac{1}{N-1} \sum_{j \epsilon N} A_{ij} \quad (6)$$

Where A is adjacency matrix with N total number of nodes in the network, and $S(i)$ is the strength or degree of node .

1.5. Brain network pattern during value learning task

In order to defined regions that are mostly involved and very important for the brain network performance, we computed the network strength and resistivity [12] from the adjacency matrix, A of each subject. A node with high strength (degree) is said to be of high hierarchy and higher impact on the system performance. Resistivity can be interpreted as opposite of functional strength which is defined as the ability of the particular node that resist the flow of network interaction and might influence brain network performance (see SI for more information).

We next investigated the regions that are less involved or indirectly involved during the value learning task. These regions might be engaged in other higher cortical activity or indirectly involved in the performance of value learning task. We, therefore computed the resistivity of a network as the effective resistance distance between two nodes in a network [12] which is based on the concept of electrical network theory, that is, the resistance of flow network interaction. The effective resistance, R(ij) between two nodes is defined as :

$$R_{ij} = \frac{detL(i,j)}{detL(i)} \quad (7)$$

Where L is the graph laplacian matrix defined by $L = D - A$. D is is the diagonal matrix of sum of matrix A, and A is the adjacency matrix of the network. L(i) is the matrix resulting from removing the ith row and column of the Laplacian and L(i,j) is the matrix resulting from removing both ith and jth rows and columns of L.

2. Supplementary results

2.1. ISC and ISFC

Some of the regions' ISC across the subjects were consistent from day to day during the the value learning task with the fusiform, lingual gyrus, occipital lobe and precentral regions were correlated across the subjects (Fig. S1A).

The correlation strength was lower in the day 4 but the lingual, fusiform gyrus and lateral occipital lobe were found to be significantly correlated across the subjects. The ISFC was lower (Fig. 2 in the main text and Fig. S1B) in the day 1 but increased in the second day with higher ISFC at the right precuneus and superior temporal pole, default mode network and visual networks. Other regions of higher ISFC include left middle temporal temporal gyrus, hippocampus, medial prefrontal cortex. In day 4, ISFC was mostly significant across the subjects in more regions that include superior and middle frontal gyri, superior parietal, angular gyrus, posterior cingulate gyrus, precuneus and cuneus, supercalcarine cortex, lateral occipital cortex, occipital fusiform gyrus, lingual gyrus, hippocampus and insular cortex.

We also computed the ISC for the rest condition for all the days (Fig. S2A and B). The average ISC was much lower during the rest condition compared to during the value learning task and statistically indistinguishable from zero. However, the ISC during rest condition was lower across all the days and ISCs for each networks or communities were similar across the days (Fig. S2B). Similarly, ISFC across the days were similar during rest condition (Fig. S2C) . Fig. S2D showed the ISFC for each brain network across the four days for resting condition.

While ISC and ISFC measure the inter-subject correlation and functional connectivity across the subjects, we established the reliability of these measures by computing the bold signal correlation and edge persistence of functional connectivity strength of each subject for three scans in each day. The bold signals of the subjects (Fig. S3A) were more correlated in the visual (VIS) system. There was higher bold signal correlation (Fig. S3B) at the lateral occipital region, lingual gyrus, and fusiform gyrus which form core part of occipital lobe, and these regions were consistent which what was observed for ISC (Fig. 2A and Fig. S1A). Other region with higher bold signal correlation are sensorimotor region and superior frontal gyrus. The average bold signal correlation (Fig. S3C) increased from day 2 to day 3 and 4 and show increase in the consistency across the scans in each day. However, edge persistence which measure the consistency of the functional connectivity strength of the three scans for each day was higher in the SM, DMN and VIS system as shown in Fig. S3D and S3E. These regions and systems are similar to what was observed in the ISFC (Fig. 2B and Fig. S1B) in day 4 which measures similarity of functional connectivity across the subjects.

2.2. Functional integration

As shown in Figure 3 in the main article, the community detection procedure yielded seven communities defined by the functional activity and structural location of the modules. The seven communities (see Table 1 in the main text) are fronto-temporal (FT), sensorimotor(SM) , default mode network (DMN), auditory (AUD), language (LAN), Visual (VIS) and the three regions putamen, caudate and thalamus (PCT). The functional connectivity pattern for each day (Fig. S4) during the task shows consistent functional connectivity pattern across the days. There were strong connections within each system most especially VIS, DMN and SM modules. The pattern of functional connectivity was consistent across the whole days and there were strong connection between the DMN, sensorimotor and visual networks which shows that these regions are more integrated than other networks during value learning task.

The functional connectivity strength increased with days as shown in Figure S5. While the average strength increased, the resistivity decreased (Fig. S5B and Fig. 5D) with days. There was significant correlation ($r \approx -1$)

between the resistivity and ISFC. Sensorimotor, lateral occipital cortex, lingual gyrus and parieto-occipital cortex had higher functional strength most especially in day 4 (Fig. S5C). Other regions include cingulate gyrus in day 2, 3 and 4 and frontal pole in day4. In contrast, the resistivity (Fig. S5C) was higher notably at the orbital frontal, parahippocampal, and inferior temporal pole that forms key part of limbic lobe especially in the third and fourth day.

References

[1] C. T. Butts, Revisiting the foundations of network analysis, science 325 (5939) (2009) 414–416.

[2] S. M. Smith, M. Jenkinson, M. W. Woolrich, C. F. Beckmann, T. E. Behrens, H. Johansen-Berg, P. R. Bannister, M. De Luca, I. Drobnjak, D. E. Flitney, et al., Advances in functional and structural mr image analysis and implementation as fsl, Neuroimage 23 (2004) S208–S219.

[3] M. W. Woolrich, S. Jbabdi, B. Patenaude, M. Chappell, S. Makni, T. Behrens, C. Beckmann, M. Jenkinson, S. M. Smith, Bayesian analysis of neuroimaging data in fsl, Neuroimage 45 (1) (2009) S173–S186.

[4] C. Torrence, G. P. Compo, A practical guide to wavelet analysis, Bulletin of the American Meteorological society 79 (1) (1998) 61–78.

[5] B. Cazelles, M. Chavez, G. C. de Magny, J.-F. Guégan, S. Hales, Time-dependent spectral analysis of epidemiological time-series with wavelets, Journal of the Royal Society Interface 4 (15) (2007) 625–636.

[6] A. Grinsted, J. C. Moore, S. Jevrejeva, Application of the cross wavelet transform and wavelet coherence to geophysical time series, Nonlinear processes in geophysics 11 (5/6) (2004) 561–566.

[7] M. Girvan, M. E. Newman, Community structure in social and biological networks, Proc. Natl. Acad. Sci. USA 99 (cond-mat/0112110) (2001) 8271–8276.

[8] P. De Meo, E. Ferrara, G. Fiumara, A. Provetti, Generalized louvain method for community detection in large networks, in: Intelligent Systems Design and Applications (ISDA), 2011 11th International Conference on, IEEE, 2011, pp. 88–93.

[9] P. J. Mucha, T. Richardson, K. Macon, M. A. Porter, J.-P. Onnela, Community structure in time-dependent, multiscale, and multiplex networks, science 328 (5980) (2010) 876–878.

[10] D. S. Bassett, N. F. Wymbs, M. A. Porter, P. J. Mucha, J. M. Carlson, S. T. Grafton, Dynamic reconfiguration of human brain networks during learning, Proceedings of the National Academy of Sciences 108 (18) (2011) 7641–7646.

[11] V. Nicosia, J. Tang, C. Mascolo, M. Musolesi, G. Russo, V. Latora, Graph metrics for temporal networks, in: Temporal networks, Springer, 2013, pp. 15–40.

[12] E. Estrada, N. Hatano, Resistance distance, information centrality, node vulnerability and vibrations in complex networks, in: Network science, Springer, 2010, pp. 13–29.

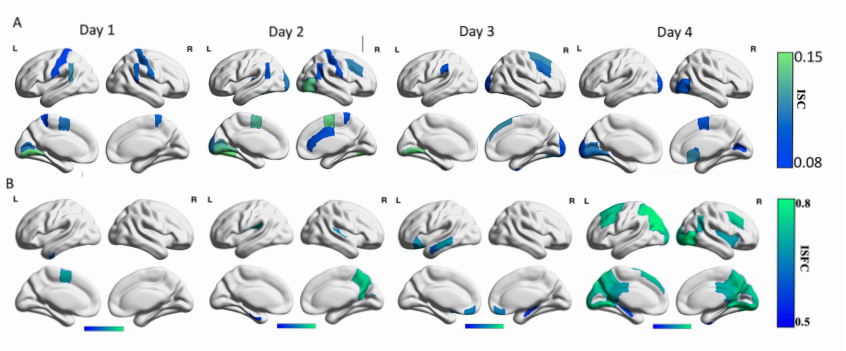

Figure 1: **ISC and ISFC maps during the task condition.** (A) ISC was consistently significant ($p < 0.05, corrected for multiple comparison$) at the lingual gyrus and sensorimotor region across the days. Other regions include supramarginal in the first three days and lateral occipital lobe in the last three days. (B) ISFC ($p < 0.05, corrected for multiple comparison$) was lower in day 1 but increased steadily with higher ISFC strength in day 3 and day 4. Regions with higher ISFC include sensorimotor, visual (higher at lingual), supramarginal, anterior cingulate gyrus and frontal pole most especially in the third and fourth day.

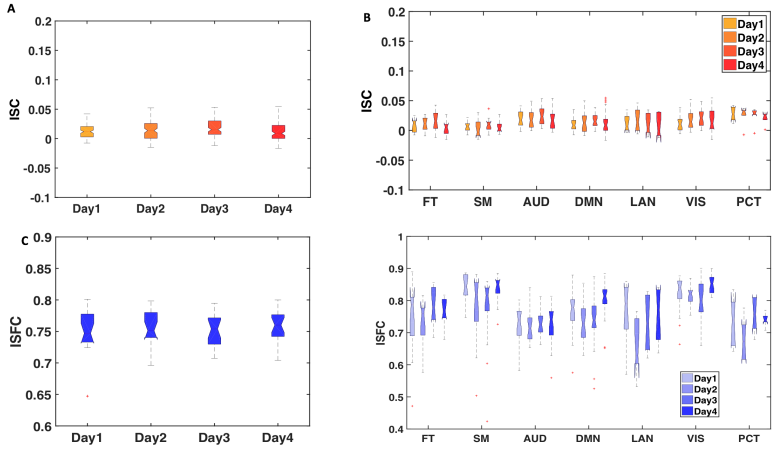

Figure 2: **ISC and ISFC during rest condition.** (A) The ISC during the rest condition is similar across the days and no obvious difference across each (B) network community. (C) The ISFC was lower in the day 2 and the same patterns were observed for all (D) the communities or networks. Fronto-temporal (FT) and auditory (AUD) networks had lower ISFC compared to other networks. Nonsignificant relationship between ISC and ISFC might due to variability across the subjects during the rest condition

Table 1: Brain regions present in the Harvard-Oxford cortical and subcortical atlas as provided by FSL

Frontal pole	Cingulate gyrus, anterior
Insular cortex	Cingulate gyrus, posterior
Superior frontal gyrus	Precuneus cortex
Middle frontal gyrus	Cuneus cortex
Inferior frontal gyrus, pars triangularis	Orbital frontal cortex
Inferior frontal gyrus, pars opercularis	Parahippocampal gyrus, anterior
Precentral gyrus	Parahippocampal gyrus, posterior
Temporal pole	Lingual gyrus
Superior temporal gyrus, anterior	Temporal fusiform cortex, anterior
Superior temporal gyrus, posterior	Temporal fusiform cortex, posterior
Middle temporal gyrus, anterior	Temporal occipital fusiform cortex
Middle temporal gyrus, posterior	Occipital fusiform gyrus
Middle temporal gyrus, temporooccipital	Fronal operculum cortex
Inferior temporal gyrus, anterior	Central opercular cortex
Inferior temporal gyrus, posterior	Parietal operculum cortex
Inferior temporal gyrus, temporooccipital	Planum polare
Postcentral gyrus	Heschl's gyrus
Superior parietal lobule	Planum temporale
Supramarginal gyrus, anterior	Supercalcarine cortex
Supramarginal gyrus, posterior	Occipital pole
Angular gyrus	Caudate
Lateral occipital cortex, superior	Putamen
Lateral occipital cortex, inferior	Globus pallidus
Intracalcarine cortex	Thalamus
Frontal medial cortex	Nucleus Accumbens
Supplemental motor area	Amygdala
Subcallosal cortex	Hippocampus
Paracingulate gyrus	Brainstem

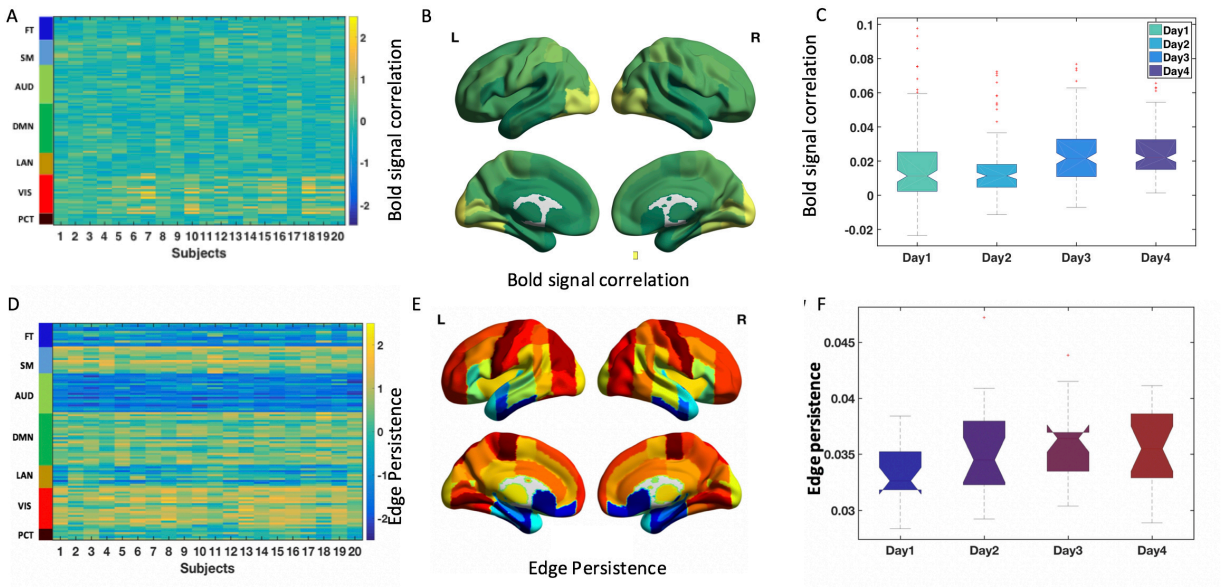

Figure 3: **Within subjects correlation during value learning task.** (A,B) Bold signal correlation (Z score) within subjects the three scans per and average across fours days revealed higher consistency at the occipital lobe especially at the lateral occipital cortex. (C) The average bold signla correlation increased as the day increases. (D) Edge persistence (zscore) across the subjects shows that SM, DMN and VIS networks had higher consistency. (E) The topological distribution of edge persistence shows higher value at the lateral occipital, lingual gyrus, pre-central and frontal lobe (F) The Edge persistence is linearly correlated with the ISFC with gradual increase and average higher value across the region at day 3.

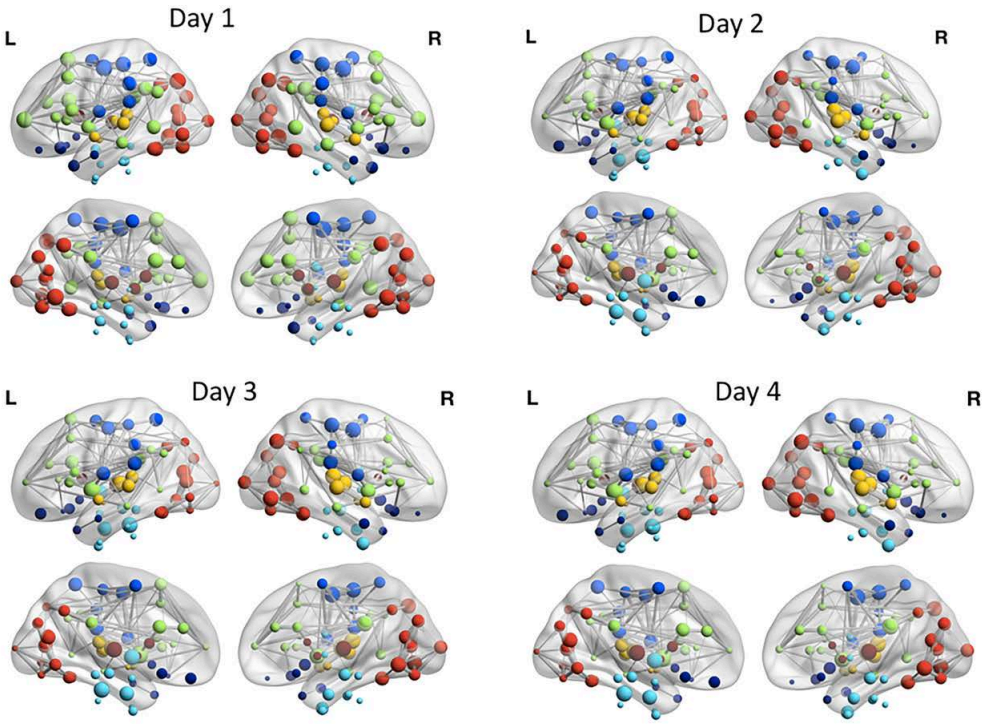

Figure 4: **Functional connectivity pattern during value learning.** Across the days, FC shows stronger connectivity (p=0.05) and higher network degree within DMN, sensorimotor and visual networks for all the days and there is interconnectivity between these networks which shows that these networks are integrated during value learning

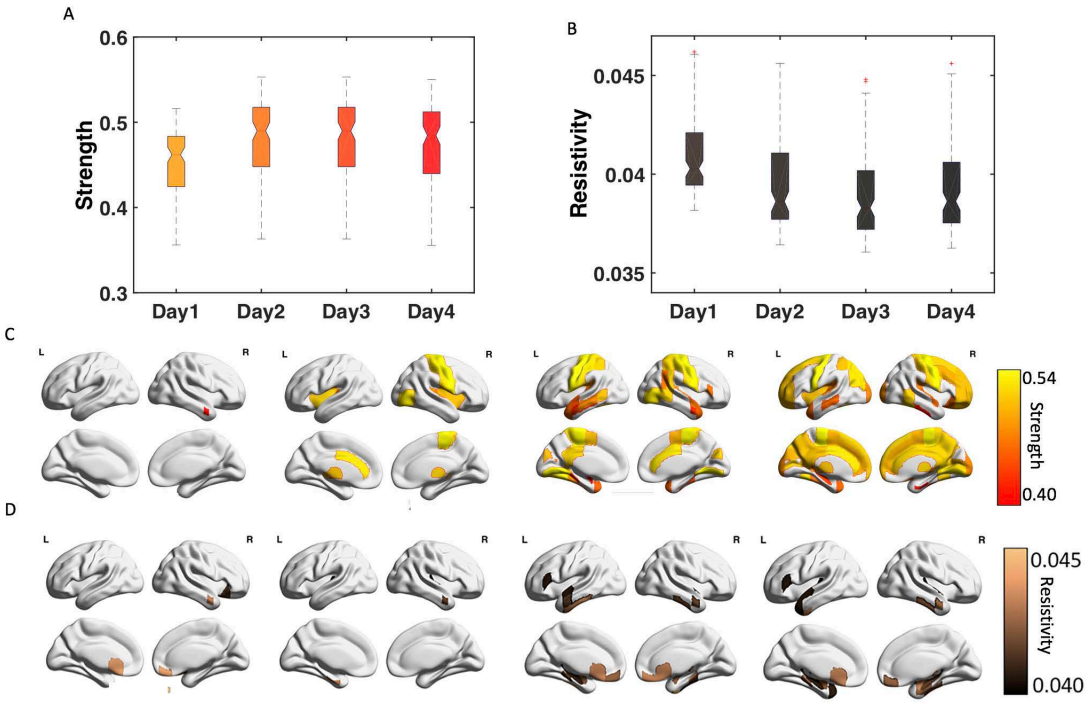

Figure 5: **Functional integration.** (A) Across the days, the strength increased with days which is directly correlated with the ISFC and accuracy while (B) the global resistivity decreased as the day increases. (C) Functional strength shows higher degree the sensorimotor region, cingulate gyrus ,cuneus and precuneus and lingual gyrus most especially in day 3 and day 4 when the functional strength was higher. (D)

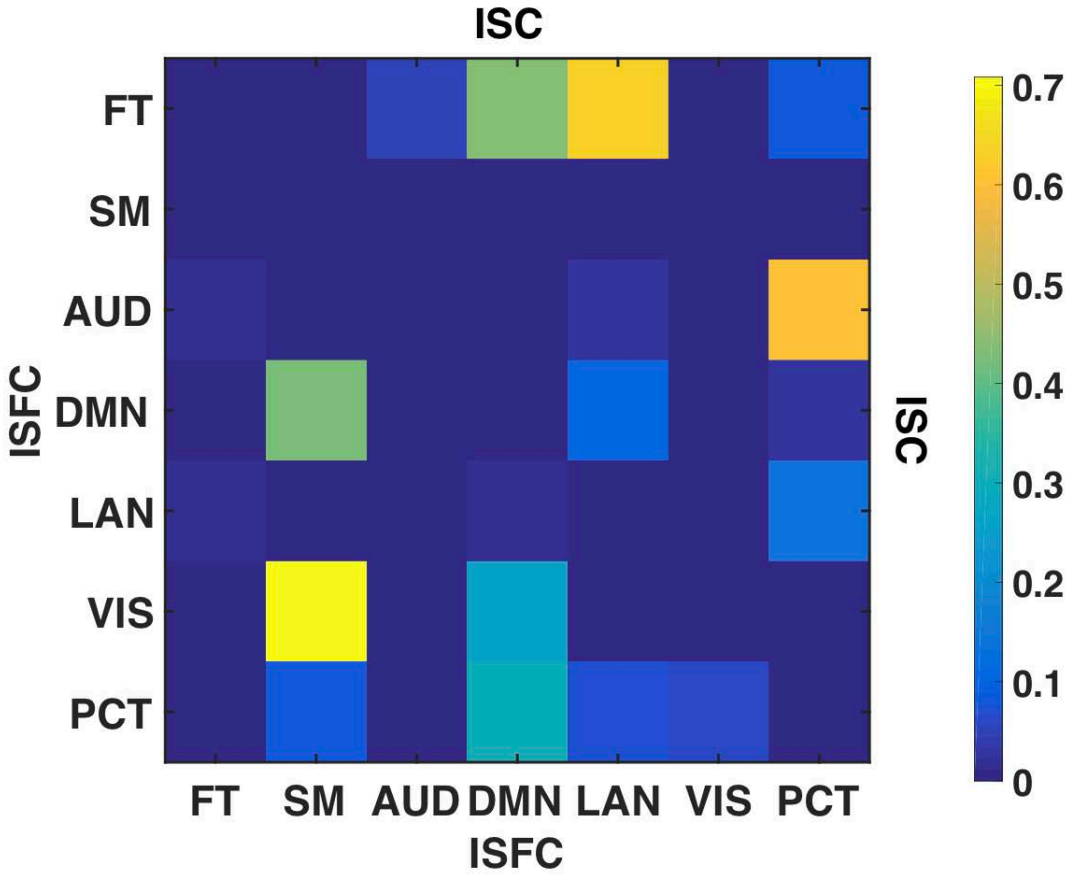

Figure 6: **Differences between the network modules for ISC and ISFC** . The matrix consist of p-values of statistical difference between pair of network communities .